Langevin Dynamics Studies of Unsaturated Phospholipids in a Membrane Environment

Linda L. Pearce and Stephen C. Harvey
Department of Biochemistry, University of Alabama at Birmingham, Birmingham, Alabama 35294 USA

ABSTRACT Computer simulations of three unsaturated phospholipids in a membrane environment have been carried out using Langevin dynamics and a mean-field based on the Marcelja model. The applicability of the mean-field to model unsaturated lipids was judged by comparison to available experimental NMR data. The results show that the mean-field methodology and the parameters developed for saturated lipids are applicable in simulations of unsaturated molecules, indicating that these simulations have good predictive capabilities. Single molecule simulations, each 100 ns in length, of 1-palmitoyl-2-oleoyl-*sn*-glycero-3-phosphocholine (POPC), 1-palmitoyl-2-elaidoyl-*sn*-glycero-3-phosphocholine (PEPC), and 1-palmitoyl-2-isolinoleoyl-*sn*-glycero-3-phosphocholine (PiLPC) reveal similarities between PEPC and DPPC. The presence of the *trans* double bond in PEPC has a minimum impact on the structural and dynamic properties of the molecule, which is probably the reason that isolated *trans* double bonds are rare in biological lipids. POPC exhibits different behavior, especially in the calculated average interchain distances, because of the *cis* double bond. The position of the two double bonds in PiLPC imparts special properties to the molecule.

INTRODUCTION

The study of phospholipids in membranes has been a difficult experimental proposition and atomic details of the motions of phospholipids are generally hard to obtain. Molecular dynamics (MD) simulations can give us a detailed view of phospholipids, but MD simulations of large systems, such as periodic boundary membrane models, are restricted to rather short time spans (picoseconds) (van der Ploeg and Berendsen, 1982, 1983; Egberts, 1988; Egberts and Berendsen, 1988). Recently, we used a mean-field approximation to study DPPC in a membrane environment and obtained interesting insight into the molecule's behavior (DeLoof et al., 1991). It was observed that tens of nanoseconds were required to bring the molecule to equilibrium and explore conformational space. It would be useful to obtain information about a variety of different types of lipids as they exist in nature in order to gain some understanding of their biological function in a membrane. To acquire this type of information about lipids for which no NMR data is available, it is necessary that the mean-field approximation adequately model unsaturated lipids and that the mean-field parameters developed for the saturated lipids are transferable to the unsaturated molecules. If no transferability exists, the predictive power of the mean-field method would be severely limited.

In an extension of the previous work, three unsaturated lipids, POPC, PEPC, and PiLPC, have been studied and the results are reported in this paper. Single molecule simulations in a mean-field were carried out on these particular lipids because there are some experimental NMR deuterium order parameters available for comparison (Seelig and Waespe-Sarcevic, 1978; Baenziger et al., 1991). This allows an evaluation of the applicability of the mean-field method to lipids with unsaturated chains.

Received for publication 23 March 1993 and in final form 11 May 1993.
Address reprint requests to Stephen C. Harvey. Tel.: 205-934-0580.

Abbreviations used: MD, molecular dynamics; POPC, 1-palmitoyl-2-oleoyl-*sn*-glycero-3-phosphocholine; PEPC, 1-palmitoyl-2-elaidoyl-*sn*-glycero-3-phosphocholine; PiLPC, 1-palmitoyl-2-isolinoleoyl-*sn*-glycero-3-phosphocholine.

0006-3495/93/09/1084/09 $2.00

METHODS

Dynamics algorithm

The method used in this paper is that previously developed by DeLoof et al. (1991). A mean-field approximation in conjunction with Langevin dynamics is used to simulate the motions of single phospholipid molecules. Simulations were carried out at 324 K, well above the phase transition temperatures of each of the lipids involved. A collision frequency of 50 ps^{-1} was used in the Langevin algorithm (Brunger et al., 1984) which was the same as used in the previous simulations of DPPC. The timestep used in all simulations was 2 fs.

Mean-Field model

The two components of the Marcelja-type mean-field (Marcelja, 1973; Schindler and Seelig, 1975; Pastor et al., 1988a) previously used for DPPC, a repulsive and a dispersive term, remained unaltered. The repulsive or steric potential is related to the surface pressure and acts on the last carbon of the lipid chain,

$$E_{rep} = \sum_{chains} \Gamma/(z_n - z_0). \quad (1)$$

The field strength, Γ, was set at −10.5 kcal-Å/mol. As the z position of the last carbon in the chain, z_n, gets closer to the lipid bilayer surface, located at z_0, force on that carbon increases and acts to pull the carbon back away from the surface.

The dispersive term (Maier-Saupe, 1959) is proportional to the molecular order parameter ((3 $\cos^2 \beta_i$ - 1)/2) and simulates the Van der Waals interactions with the surrounding lipid molecules:

$$E_{disp} = \sum_{\text{chain carbons}} - \Phi(1/2)(3 \cos^2\beta_i - 1) \qquad (2)$$

The field strength, Φ, was set to 0.21 kcal/mol as in the DPPC simulations. For an sp^3 carbon, β_i is the angle between the bilayer normal and the vector normal to a plane spanned by the two C-H vectors. For the sp^2 carbon, β_i is the angle between the bilayer normal and the vector normal to the C-H vector contained in the plane defined by the carbons involved in the double bond and the hydrogen bound to the carbon under investigation.

A surface potential at −4 Å was used to keep the ends of the acyl chains from moving out into the bilayer, and the phosphorous atom was fixed to the origin of the coordinate system by a harmonic constraint. The nitrogen atom of the choline headgroup was also constrained to the *x-y* plane to mimic the bilayer surface. Details of these constraints can be found in DeLoof et al. (1991) and were not varied in this study.

Starting structures and force potentials

The starting structures of PEPC, POPC, and PiLPC were derived from the united atom structure of DPPC previously used. The new structures were equilibrated for 300 ps prior to the start of data collection. The potential function parameters were primarily taken from the AMBER (Weiner et al., 1984) and CHARMm (Brooks et al., 1983) force fields. Nonbonded interactions included only a 6–12 Lennard Jones potential (cutoff, 8 Å) and no electrostatics. Standard torsion potentials were used except for the sp^3-sp^3 carbon torsions where the Ryckaert-Bellmans potential (1975) was used.

Calculation of simulation results

The deuterium order parameter is given by:

$$S_{CD} = \tfrac{1}{2}\langle 3 \cos^2\theta - 1\rangle, \qquad (3)$$

where θ is the angle between the vector along the carbon-deuterium bond and the bilayer normal. S_{CD} values were calculated every 10 steps, and the time averages were compared to experimental results. Convergence of the simulations was checked by following the deuterium order parameters.

Coordinate statistics and correlation functions

Coordinates were saved every picosecond. Autocorrelations were calculated with the use of fast Fourier-transform routines (Press et al., 1988). The reorientational correlation functions $\langle P_2[\mu(t) \cdot \mu(0)]\rangle$ for selected unit vectors $\mu(t)$ were obtained using the $l = 2$ spherical harmonic correlation functions (see also Pastor et al., 1988b). The relaxation times used the first 5000 ps of data and generally needed two exponentials to give the best fits.

Computer resources

All programs were written in the C language by H. DeLoof and were based on the yammp package (Tan and Harvey, 1993). Calculations were performed on a solitary processor in a hybrid Silicon Graphics 4D/340-GTX machine. 1 ns of simulation of one phospholipid molecule took about 2 h.

RESULTS

In Fig. 1 are shown the deuterium order parameters of the *sn*-2 chain for PEPC, POPC, and PiLPC simulations along with those experimentally determined by Seelig and Waespe-Sarcevic (1978) and Baenziger et al. (1991). The simulations were 100-ns long, and the deuterium order parameters for the C2 carbons on all chains took the longest to converge. It has been previously observed (DeLoof et al., 1991) that such a long simulation time (100 ns) is necessary to span conformational space and reach equilibrium. Fairly good agreement between our simulated results and the experimental data is obtained. Importantly, very good agreement between simulation and experiment is noted in the area of the double bonds. There are some larger differences in the first few carbons in the chain which are probably due to the repulsive surface that models the bilayer interface. Also, the order parameters are somewhat larger near the ends of the chain in the simulated data than those obtained by NMR experiment. This may be a consequence of the repulsive force which pulls on the ends of the chain. Overall, however, the agreement between simulation and experiment is fairly convincing.

The deuterium order profiles of the *sn*-1 chain simulations of PEPC, POPC, and PiLPC are very similar to those obtained experimentally for DPPC, although slightly more disorder is noted. Those values derived from the simulation of POPC show even more disorder near the first half of the chain. This indicates that the double bonds in the *sn*-2 chains also affect the motions of the *sn*-1 chains.

The average lengths of each of the chains in the simulations of POPC, PiLPC, and PEPC along with DPPC are shown in Table 1. The 16-carbon unsaturated *sn*-1 chains are similar, but the *sn*-1 chain length decreases as the *sn*-2 chain goes from being saturated to containing a *trans* double bond, then *cis*, and finally two *cis* double bonds. Again we note

Table 1 Average *sn*-1 and *sn*-2 chain lengths from computer simulations

	Molecule			
	DPPC*	PEPC	POPC	PiLPC
		Å		
sn-1 chain	18.13	18.00	17.52	17.20
sn-2 chain	17.84	17.75	16.65	16.72

* DeLoof et al. (1991).

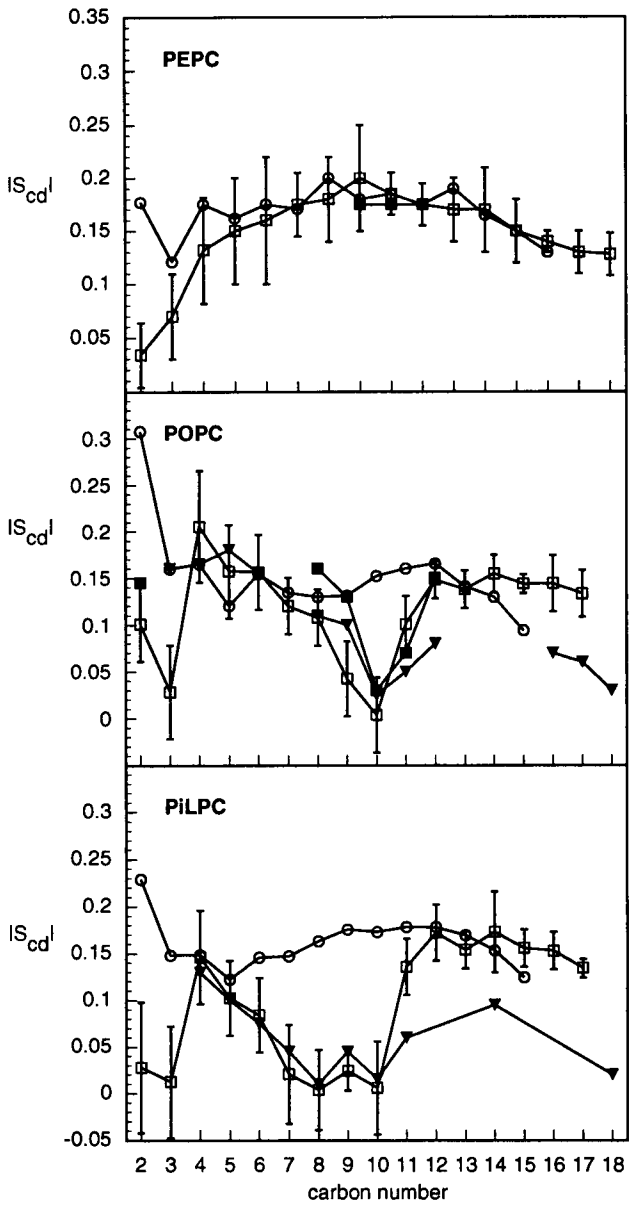

FIGURE 1 Deuterium NMR order parameters for 100-ns simulations of PEPC, POPC, and PiLPC with experimental data of Seelig and Waespe-Sarcevic (1978) and Baenziger et al. (1991). Experimental values of the *sn*-2 chain from Baenziger et al. (1991) are shown with solid triangles; experimental values of Seelig and Waespe-Sarcevic (1978) are shown with solid squares. Open squares represent the order parameters of the *sn*-2 chain calculated from the simulations; open circles represent the order parameters of the *sn*-1 chain from the simulations. Simulation data are the averages of both hydrogens on the sp^3 carbons. Standard deviations (square roots of the fluctuations) are shown for the *sn*-2 chains.

some effect of the *sn*-2 chain on the *sn*-1 chain. A similar trend in chain length is noted for the *sn*-2 chain. The attachment of the *sn*-2 chain to the second carbon of the glycerol backbone of the phospholipid causes a kink in the *sn*-2 chain which gives rise to the shorter chain lengths compared to the *sn*-1 chain. It must be noted that the *sn*-2 chain of the POPC molecule which contains a single *cis* double bond is approximately the same length as the *sn*-2 chain in PiLPC, containing two double bonds in the *cis* conformation.

Fig. 2 shows the probability distribution for the *z* coordinates of the oxygen and carbon atoms of the *sn*-2 chains of PEPC, POPC, and PiLPC. The keto oxygen, the carbonyl carbon, and oxygen show a narrow distribution profile in comparison with the carbons in the acyl chain. Each carbon shows a progressively larger range of motions in the *z* direction proceeding toward the terminal carbons. However, there does appear to be a slight narrowing of the distribution profile near the center of the molecules in the vicinity of the double bonds. POPC also seems to exhibit a different behavior in that the carbons involved in the double bond (9, 10) and those adjacent also occupy space near the membrane surface in a bimodal manner. This also occurs for the carbon in the sixth position (the beginning of the double bond) of PiLPC.

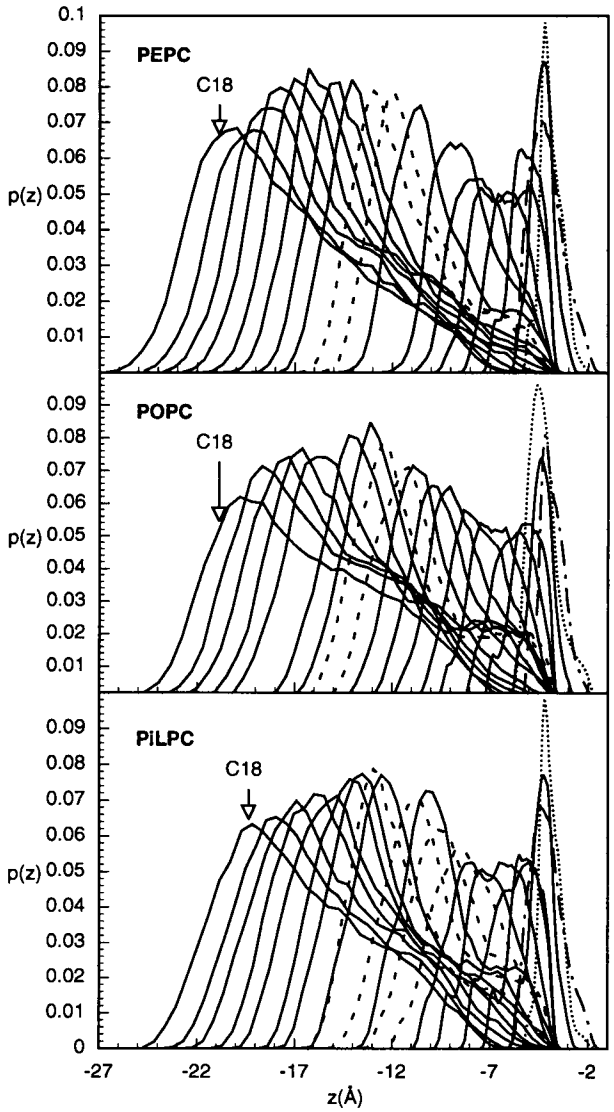

FIGURE 2 Probability distribution for the *z* coordinates of the oxygen and carbon atoms of the *sn*-2 chains of PEPC, POPC, and PiLPC. Dashed lines represent the carbons involved in double bonds. Dotted lines represent the ether oxygen. Broken lines represent the carbonyl oxygen. Solid lines represent the acyl carbons.

The transition rates of the torsion angles have been investigated and are shown in Fig. 3. First, it is noted that the rates observed for all the *sn*-1 chains are nearly identical and virtually superimposable with those previously obtained for DPPC. Away from the ends of the *sn*-1 chains a plateau effect indicates, as previously observed (DeLoof et al., 1991), that annealing around the new conformation is the principle isomerization mechanism. Thus, the differences observed for the *sn*-1 chains in the deuterium NMR order profiles are probably not due to a change in the torsion transition rates.

Transition rates in the *sn*-2 chains are quite different, however. In the case of the single double bond in the *trans* conformation, large increases are observed in both the *trans* → *gauche* and *gauche* → *trans* isomerization rates immediately preceding and following the unchanging double bond torsion. A slight decrease in the rates preceding and following those torsions is also observed. There is a greater fraction of *gauche* torsions surrounding the *trans* double bond than is seen in the saturated system (DeLoof et al., 1991), 0.314 vs. 0.274.

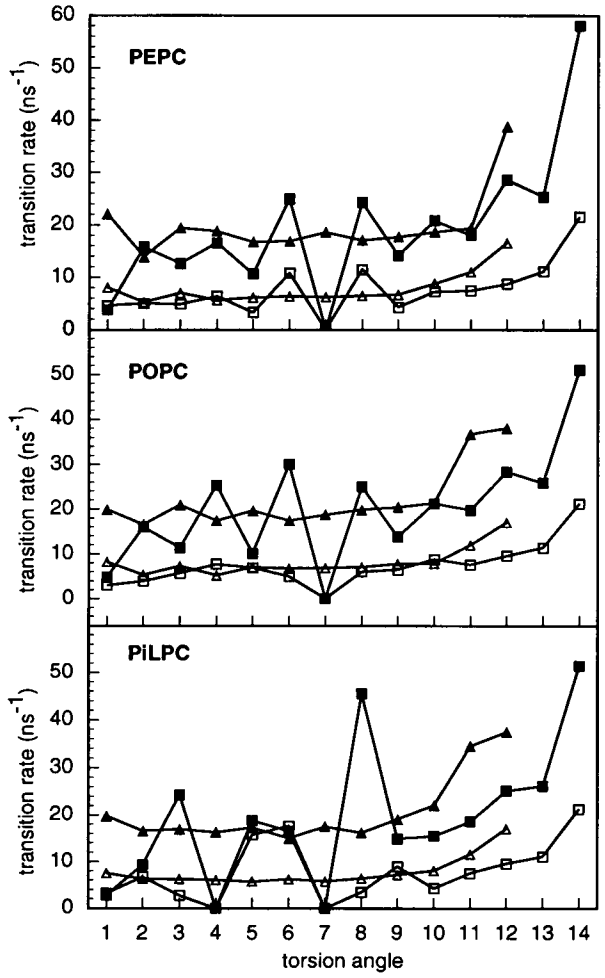

FIGURE 3 Transition rates of the torsion angles of both chains of PEPC, POPC, and PiLPC estimated by using the "simple counting" procedure (Longcharich, et al., 1992). The first torsion corresponds to the one between C3 and C4. Open symbols, *trans-gauche* rates; solid symbols, *gauche-trans* rates; triangles, *sn*-1 chain rates; squares, *sn*-2 chain rates.

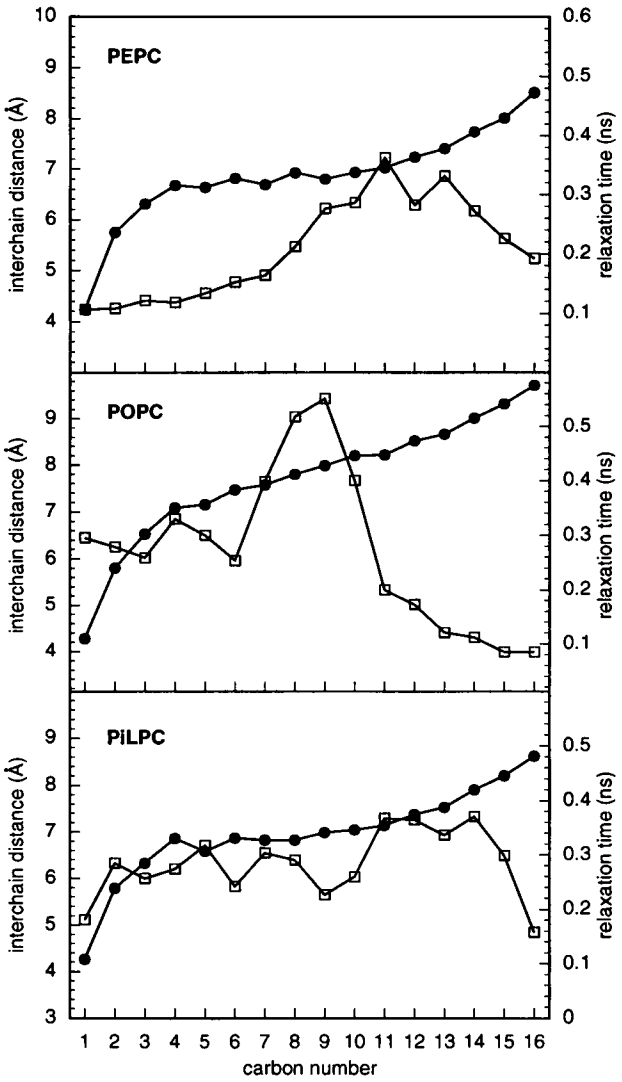

FIGURE 4 Average interchain distances (*solid circles*) and associated relaxation times (*open squares*) for the simulations of PEPC, POPC, and PiLPC. The relaxation times are weighted averages based on two exponential fits of the interchain distance autocorrelation function, $\tau = (a_1\tau_1 + a_2\tau_2)/(a_1 + a_2)$.

The situation for the single *cis* double bond is similar but the *trans* → *gauche* rates decrease rather than increase. Those torsions adjacent to the *cis* double bond exhibit a much higher proportion of torsion angles in the *trans* conformation, 0.910, than observed for the saturated acyl chains (DeLoof et al., 1991), 0.726. The *gauche* → *trans* transition rates for the torsion preceding the *cis* double bond at the sixth position and the torsion immediately following the double bond at the ninth position in the *sn*-2 chain of PiLPC also increase. However, between the two double bonds, the *trans* → *gauche* and *gauche* → *trans* rates for those two torsions are near an equilibrium value of one, the largest increase being for the *trans* → *gauche* torsion transition rate. These transition rates reflect the influence of the geometry of the nearby double bonds. We also observe a general reduction in transition rates for the torsion angles toward the ends of all the *sn*-2 chains

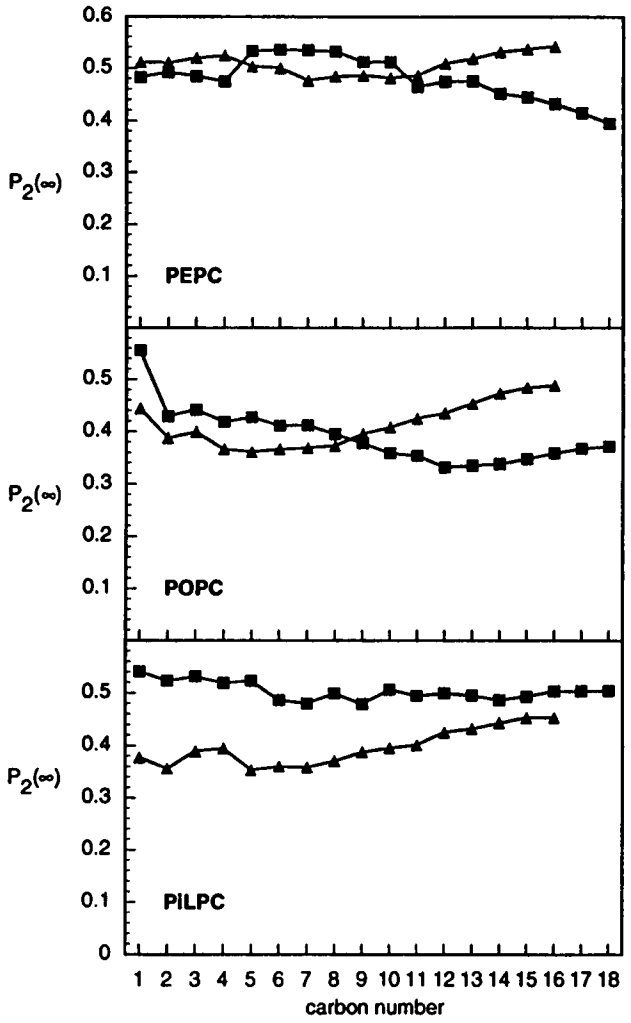

FIGURE 5 Limiting value of the P_2 autocorrelation function of the vector from the phosphorous atom to the carbon atoms in the *sn*-1 chain (*triangles*) and to the *sn*-2 chain (*squares*) for PEPC, POPC, and PiLPC.

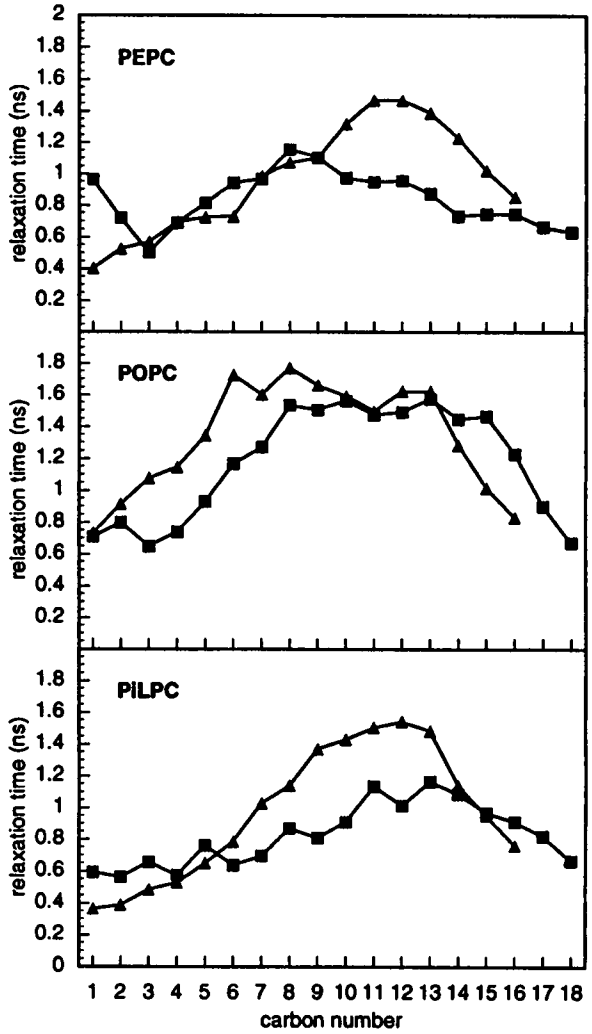

FIGURE 6 Relaxation times are weighted averages based on two exponential fits, $\tau = (a_1\tau_1 + a_2\tau_2)/(a_1 + a_2)$, for the vectors described in Fig. 5 of PEPC, POPC, and PiLPC. The values for the *sn*-1 chains are represented by triangles and the *sn*-2 chains are represented by squares.

compared with the *sn*-1 chains. That is, an extension of the plateau region in transition rate is observed due to the addition of two carbons to the *sn*-2 chain along with a large increase in rate for the final torsion angle. This increase in transition rate for the terminal *sn*-2 carbons does not appear to affect the order parameters at the ends of the chain. While it may be argued that increases in torsion angle transition rates for POPC and PiLPC in the vicinity of the double bonds parallel the decrease in order parameter, this is certainly not true for PEPC.

A very interesting result is obtained when the average interchain distance between equivalent carbon atoms on the *sn*-1 and *sn*-2 chains is calculated (Fig. 4). The average distances of PEPC and PiLPC are nearly identical, and the two *sn*-1 and *sn*-2 chains are marginally further apart than those of DPPC. However, note that in POPC the two chains begin to separate more starting at the carbons in the fifth position and are nearly an angstrom further apart at the ends of the chains than those of PEPC and PiLPC. The relaxation time needed to reach these distances is also shown in Fig. 4. These are calculated using the autocorrelation function and then fitting the data with exponentials. The parameters for these fits were obtained by a grid search followed by the Levenberg-Marquart method (Press et al., 1988). The decays are somewhat complicated and generally a two exponential fit was a slight improvement over a single exponential fit. The results of the two exponential fits are shown in Fig. 4. Each of the unsaturated lipids studied produced a slightly different relaxation profile. In general the relaxation times observed for PEPC parallel those previously observed for DPPC but the times are somewhat shorter than those seen for DPPC. PiLPC exhibits slightly longer relaxation times at the beginning of the chains and does not have the large increase in relaxation time at the tenth carbons. POPC again exhibits quite different behavior. The relaxation times are quite long prior to the single *cis* double bond and become remarkably shorter after the double bond, almost the opposite behavior observed for the molecule containing the single *trans* double bond, PEPC.

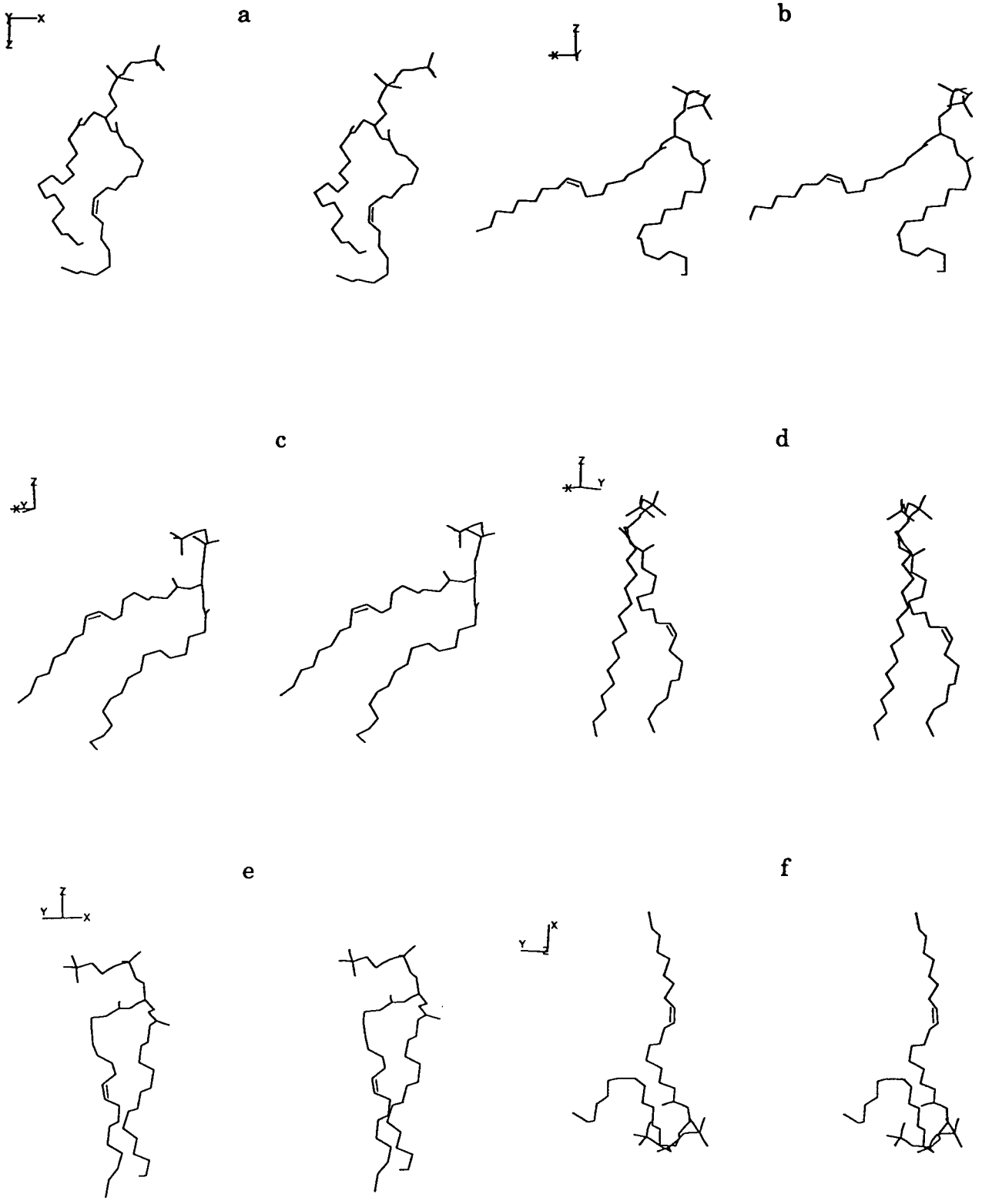

FIGURE 7 Representative structures of POPC. The x-y plane is parallel to the lipid/solvent interface. f is a top view.

The two motions previously used to describe the relaxation mechanism were torsion angle transition (shorter relaxation times) and wobbling motions of the individual chains (longer relaxation times). This suggests that the torsion angle transitions are important for the relaxation mechanism near the ends of the chain and perhaps near the double bonds (PEPC and PiLPC). The longer relaxation time near the double bond in POPC indicates that the wobbling motions and the geometry may be the more important factors in the relaxation mechanism in this part of the molecule followed by almost

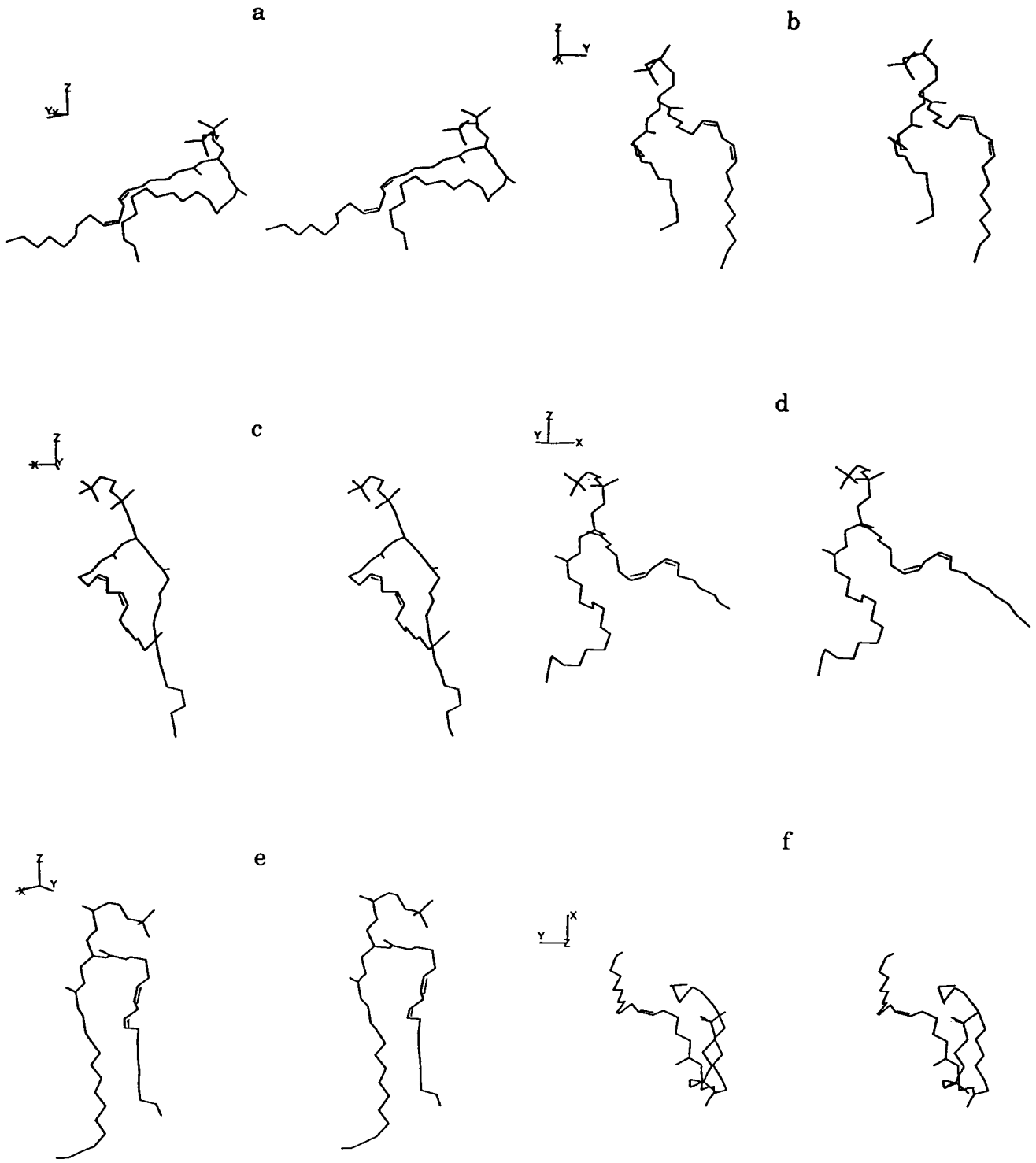

FIGURE 8 Representative structures of PiLPC. The *x-y* plane is parallel to the lipid/solvent interface. *f* is a top view.

all torsional relaxation at the ends of the POPC chains. The *sn*-2 chain of POPC appears to be "elbowing" the *sn*-1 chain in the same molecule.

In Fig. 5 the equilibrium values, $P_2(\infty)$ calculated from the P_2 correlation function for the vector from the phosphorous atom to each individual carbon in the *sn*-1 and *sn*-2 chains of PEPC, POPC, and PiLPC are shown. This gives some measure of the global motions of these molecules in a membrane. It can be seen that the three are fairly similar. In Fig. 6 are shown relaxation times based on two exponential fits of the autocorrelation function decays. Again these are similar (especially PiLPC and PEPC) and exhibit long relaxation times (up to 1.5 ns). The longer relaxation times for all of the carbon atoms are probably due to wobbling and rotational

motions. Only a slight increase in the relaxation times for the first half of the POPC chains is seen and again slightly overall longer relaxation times for the *sn*-2 chain of POPC.

DISCUSSION

The primary aim of this work was to evaluate the general applicability of the recently developed mean-field method to unsaturated acyl chains and the transferability of the mean-field parameters to unsaturated molecules. As a first criterion the experimental NMR order parameter profiles should be replicated by the Langevin dynamics simulations. As was shown in Fig. 1, this requirement was fairly well met. The mean-field parameters used in simulating the unsaturated phospholipids were precisely the same as those used in simulating DPPC, a saturated phospholipid. While some improvements in replicating the order parameters may be forthcoming (by using the stochastic boundary method developed by DeLoof et al. (1991)) the present method should be useful in predicting the acyl chain motions of a variety of lipids in a membrane.

Having demonstrated the viability of the mean-field and the transferability of the mean-field parameters in studying unsaturated lipids in a membrane environment, numerous interatomic details have been probed. It is fairly clear that PEPC very closely resembles DPPC in most of its attributes. Thus, one can rationalize the general lack of *trans* double bonds appearing in nature. The presence of a *trans* double bond does not influence the behavior of the chain much, as the torsions in an saturated chain prefer a mostly *trans* geometry.

Seelig and Waespe-Sarcevic (1978) first suggested that POPC mainly differs from PEPC in its NMR behavior due to the geometry about the double bond (*cis* versus *trans*). All the data in this paper support this view. The *trans* bond elicits an opposite sp^2-sp^3 torsion transition rate effect from that observed by a *cis* double bond. That is, a greater proportion of *trans* conformations are observed near the *cis* double bond and a greater proportion of *cis* conformations are observed near the *trans* double bond. Rey et al. (1992) have seen similar phenomena in a Brownian dynamics study of unsaturated chains. Rey et al. (1992) suggested that *gauche plus* $\leftrightarrow$ *gauche minus* transitions were important in unsaturated chain dynamics, but none were observed in this current study as the Rykaert-Bellmans potential has a high barrier to the transition. The overriding factor in the NMR order profile appears to be the geometry of the deuterium attached to the double bond rather than the torsion transition rate. The *cis* double bond acts as a "kink" or "elbow" in the acyl chain. The chain above and below the double bond tends to be in the *trans* or extended conformation. This results in the elbow-like structures observed. The *sn*-2 acyl chain with its kink then elbows the *sn*-1 chain and forces it to adopt conformations similar to that seen in Fig. 7 *a*. This elbowing of the *sn*-1 chain causes a greater disorder in the chain as observed by the NMR order parameters compared with a saturated lipid *sn*-1 chain. The double bond also tends to spend some time near the surface as this allows the end of the chain to remain in the extended conformation.

Another interesting result is the similarity observed between the unsaturated chains and PiLPC, particularly the interchain distance. The interchain distance relaxation phenomena does show some differences, however. Clearly the torsion transitions are more important in PEPC and DPPC than PiLPC where wobbling appears to be a larger part of the interchain relaxation mechanism. Previous data on DPPC indicated that the two chains did not move independently. It is clear that *cis* double bonds do cause greater disorder in the *sn*-1 chain as evidenced from the simulated deuterium NMR profiles. The first *cis* double bond in PiLPC causes the acyl chain to act in a similar fashion to POPC but the "elbow " is now shorter. The flexibility at the sp^3 carbon between the two double bonds allows the second double bond to curl back toward the *sn*-1 chain. A result is the interchain distances which are similar to DPPC and PEPC. This can be observed by the representative structures in Fig. 8. Thus, the position and flexibility between the two double bonds do not create as great a disruption as the one double bond in POPC, as might be expected from the appearance of the NMR data.

CONCLUSIONS

Detailed observation of the properties of unsaturated lipids in membranes are possible with the methodology developed by DeLoof et al. (1991). Both the mean-field approach and the specific parameters developed for saturated lipids are transferable to simulations of unsaturated molecules. This is an important result, because the predictive power of this method would be undermined if we had to reparameterize the mean-field for each kind of molecule; we would only be able to simulate systems for which NMR order parameters are available.

Another important result is the fact that PEPC very closely resembles DPPC in most of its attributes. That is, the presence of a *trans* double bond has little influence on the behavior of the chain, as the torsions in an saturated chain prefer a mostly *trans* geometry. Surely this suggests that a reason the *trans* double bond is so rarely found in biological lipids is that it is redundant.

It is possible that better results may be obtained using the mean-field stochastic boundary molecular dynamics method and these simulations as well as calculations of T_1 relaxation times for comparison to NMR are underway. This study also gives confidence in the predictive power of the method and simulations of highly unsaturated docosahexaenoyl chains are underway in order to give some insight into the angle-iron and helix conformations proposed by Applegate and Glomset (1986).

We particularly thank Jere Segrest, Michael R. McBride, and Paul Konstant for helpful discussions.

This work was supported by grant 2P01HL34343 from the National Institutes of Health.

REFERENCES

Applegate, K. R., and J. A. Glomset. 1986. Computer-based modeling of the conformation and packing properties of docosahexaenoic acid. *J. Lipid Res.* 27:658–680.

Baenziger, J. E., H. C. Jarrell, R. J. Hill, and I. C. P. Smith. 1991. Average structural and motional properties of a diunsaturated acyl chain in a lipid bilayer: effects of two *cis*-unsaturated double bonds. *Biochemistry.* 30: 894–903.

Brooks, B. R., R. E. Bruccoleri, B. D. Olafson, D. J. States, S. Swaminathon, M. Karplus. 1983. CHARMM: a program for macromolecular energy, minimization and dynamics calculations. *J. Comp. Chem.* 4:187–217.

Brunger, A., C. B. Brooks, and M. Karplus. 1984. Stochastic boundary conditions for molecular dynamics simulations of ST2 water. *Chem. Phys. Lett.* 105:495–498.

DeLoof, H., S. C. Harvey, J. P. Segrest, and R. W. Pastor. 1991. Mean field stochastic boundary molecular dynamics simulation of a phospholipid in a membrane. *Biochemistry.* 30:2099–2113.

Egberts, E. 1988. Molecular dynamics simulation of multibilayer membranes. Ph.D. thesis. Rijksuniversiteit, Groningen.

Egberts, E., and H. J. C. Berendsen. 1988. Molecular dynamics simulation of a smectic liquid crystal with atomic detail. *J. Chem. Phys.* 89:3718–3726.

Loncharich, R. J., B. R. Brooks, and R. W. Pastor. 1992. Langevin dynamics of peptides: the frictional dependence of isomerization rates of *N*-acetylalanyl-*N'*-methylamide. *Biopolymers.* 32:523–535.

Maier, W., and Saupe, A. 1959. Eine einfache molecular-statictsche kristallinflussigen phase: teil I. *Z. Naturforsch. A.* 14:882–889.

Marcelja, S. 1973. Molecular model for phase transition in biological membranes. *Nature (Lond.).* 241:451–452.

Pastor, R. W., R. W. Venable, and M. Karplus. 1988a. Brownian dynamics simulation of a liquid chain in a membrane bilayer. *J. Chem. Phys.* 89: 1112–1227.

Pastor, R. W., R. W. Venable, M. Karplus, and A. Szabo. 1988b. A simulation based model of NMR T_1 relaxation in lipid bilayer vesicles. *J. Chem. Phys.* 89:1128–1140.

Press, W. H., B. P. Flannery, S. A. Teukolsky, and W. T. R. Vetterling. 1988. Numerical recipes in C: the art of scientific computing. Cambridge University Press, Cambridge.

Rey, A., A. Kolinski, J. Skolnick, and Y. K. Levine. 1992. Effect of double bonds on the dynamics of hydrocarbon chains. *J. Chem. Phys.* 97:1240–1249.

Ryckaert, J. P., and A. Bellmans. 1975. Molecular dynamics of liquid *n*-butane near its boiling point. *Chem. Phys. Lett.* 30:123–125.

Schindler, H., and J. Seelig. 1975. Deuterium order parameters in relation to thermodynamic properties of a phospholipid bilayer: a statistical mechanical interpretation. *Biochemistry.* 14:2283–2287.

Seelig, J., and N. Waespe-Sarcevic. 1978. Molecular order in *cis* and *trans* unsaturated phospholipid bilayers. *Biochemistry.* 17:3310–3315.

Tan, R. K.-Z., and S. C. Harvey. 1993. YAMMP: the development of a molecular modeling program using the modular programming method. *J. Comp Chem.* 14:455–470.

der Ploeg, P., and H. J. C. Berendsen. 1982. Molecular dynamics simulation of a bilayer membrane. *J. Chem. Phys.* 76:3271–3276.

der Ploeg, P., and H. J. C. Berendsen. 1983. Molecular dynamics of a bilayer membrane. *Mol. Physiol.* 49:233–248.

Weiner, S. J., P. A. Kollman, D. A. Case, U. C. Singh, C. Ghio, G. Alagona, S. Profeta, and P. Weiner. 1984. A new force field for molecular mechanical simulation of nucleic acids and proteins. *J. Am. Chem. Soc.* 106:765–784.